Strong decays of heavy-light mesons in a chiral quark model

Xian-Hui Zhong[1,3,*] and Qiang Zhao[1,2,3,+]

[1]*Institute of High Energy Physics, Chinese Academy of Sciences, Beijing 100049, People's Republic of China*
[2]*Department of Physics, University of Surrey, Guildford, GU2 7XH, United Kingdom*
[3]*Theoretical Physics Center for Science Facilities, Chinese Academy of Sciences, Beijing 100049, People's Republic of China*

(Received 2 April 2008; revised manuscript received 30 May 2008; published 31 July 2008)

We carry out a systematic study of the heavy-light meson strong decays in a chiral quark model. For the S-wave vectors [$D^*(2007)$, $D^{*\pm}(2010)$], P-wave scalars [$D_0^*(2400)$, $B_0^*(5730)$], and tensors [$D_2^*(2460)$, $D_{s2}^*(2573)$], we obtain results in good agreement with the experimental data. For the axial vectors $D_1(2420)$ and $D_1'(2430)$, a state mixing scheme between 1^1P_1 and 1^3P_1 is favored with a mixing angle $\phi \simeq -(55 \pm 5)^\circ$, which is consistent with previous theoretical predictions. The same mixing scheme also applies to $D_{s1}(2460)$ and $D_{s1}(2536)$ that accounts for the narrow width of the $D_{s1}(2536)$ and its dominant decay into D^*K. For $B_1(5725)$ and $B_1'(5732)$, such a mixing explains well the decay width of the former but leads to an even broader $B_1'(5732)$. Predictions for the strange-bottom axial vectors are also made. For the undetermined meson $D^*(2640)$, we find that they fit well in the radially excited state 2^3S_1 according to its decay mode. The newly observed $D_{sJ}^*(2860)$ strongly favors the D-wave excited state 1^3D_3. For $D_{sJ}^*(2632)$ and $D_{sJ}^*(2690)$, we find they are difficult to fit in any D_s excitations in that mass region, if the experimental data are accurate. Theoretical predictions for decay modes of those unobserved states as multiplets of $2S$ and $1D$ waves are also presented, which should be useful for the further experimental search for those states.

DOI: 10.1103/PhysRevD.78.014029 PACS numbers: 12.39.Fe, 12.39.Jh, 13.25.Ft, 13.25.Hw

I. INTRODUCTION

During the past several years, significant progress has been made in the observation of the heavy-light mesons. In 2003, two new narrow charm-strange mesons $D_{sJ}^*(2317)$ and $D_{sJ}^*(2460)$ were observed by *BABAR*, CLEO, and Belle [1–5]. Recently, *BABAR* reported another two new charm-strange mesons, i.e. $D_{sJ}^*(2860)$ with a width of (47 ± 17) MeV and $D_{sJ}^*(2690)$ with a width of (112 ± 43) MeV in the DK decay channel [6]. Meanwhile, Belle reported a new vector state $D_{sJ}^*(2708)$ with a width of $(108 \pm 23^{+36}_{-31})$ MeV [7]. The $D_{sJ}^*(2690)$ and $D_{sJ}^*(2708)$ are believed to be the same state since their masses and widths are consistent with each other. In the B meson sector two narrow states $B_1(5725)$ and $B_2^*(5740)$ were reported by CDF [8], and are assigned as orbitally excited B mesons. They were confirmed by the D0 Collaboration with slightly different masses [9]. The CDF Collaboration also reported their strange analogues, $B_{s1}(5829)$ and $B_{s2}^*(5840)$, as orbitally excited B_s mesons [10]. The $B_{s2}^*(5840)$ is also observed by the D0 Collaboration [11]. About the recent experimental status of the heavy-light mesons, many reviews can be found in Refs. [12–18].

To understand the nature of the heavy-light mesons, especially the newly observed states, and to establish the heavy-light meson spectroscopy, a lot of effort has been put into both experiment and theory. For example, one can find recent discussions about the dynamics and decay properties of the heavy-light mesons given by Close and Swanson [19], Godfrey [20], and other previous analyses in Refs. [21–32]. For the new observed heavy-light mesons, such as $D_{sJ}^*(2860)$ and $D_{sJ}^*(2690)$, various attempts on the explanation of their nature have been made [33–43]. Many systematic studies are devoted to establishing the D, D_s, B, and B_s spectroscopies [44–49], while some earlier work can be found in Refs. [21,50]. Recent reviews of the status of the theory study of the heavy-light mesons can be found in Refs. [51–58].

On the one hand, the improved experimental measurements help clarify some old questions on the spectrum. On the other hand, they also raise some new ones which need further experimental and theoretical study [59,60]. For instance, $D^*(2640)$ reported by DELPHI in $D^{*+}\pi^+\pi^-$ [61] as the first radial excited state still has not yet been confirmed by any other experiments. The spin-parity of the narrow $D_1(2420)$ also needs confirmation. The status of the broad $D_0^*(2400)$ is not clear at all: its measured mass and width have uncertainties that are too large. For the D_s spectroscopy, the low masses of the $D_{sJ}^*(2317)$ and $D_{sJ}^*(2460)$ still cannot be well explained by theory; whether they are exotic states is an open question. Theoretical predictions for the $D_{sJ}^*(2860)$ and $D_{sJ}^*(2690)$ are far from convergence. The narrow state $D_{sJ}^*(2632)$ seen by the SELEX Collaboration [62] cannot be naturally explained by any existing theory. Nevertheless, since the flavor symmetry of the heavy-light mesons is badly broken, a mixture of states with the same J^P may occur. This will add further complexities into the meson spectrum, and further theoretical investigationis needed.

*zhongxh@ihep.ac.cn
+zhaoq@ihep.ac.cn

In this work, we make a systematic study of the strong decays of heavy-light mesons in a chiral quark model. In the heavy-quark infinite mass limit, the flavor symmetry no longer exists in the heavy-light mesons, which allows us to describe the initial and final D, D_s, B, and B_s mesons in a nonrelativistic framework self-consistently. The meson decay will proceed through a single-quark transition by the emission of a pseudoscalar meson. An effective chiral Lagrangian is then introduced to account for the quark-meson coupling. Since the quark-meson coupling is invariant under the chiral transformation, some of the low-energy properties of QCD are retained. This approach is similar to that used in Refs. [21,22], except that the two constants in the decay amplitudes of Refs. [21,22] are replaced by two energy-dependent factors deduced from the chiral Lagrangian in our model.

The chiral quark model approach has been well developed and widely applied to meson photoproduction reactions [63–71]. Its recent extension to describe the process of πN scattering and investigate the strong decays of charmed baryons also turns out to be successful and inspiring [72,73].

The paper is organized as follows. In the subsequent section, the heavy-light meson in the quark model is outlined. Then, the nonrelativistic quark-meson couplings are given in Sec. III. The decay amplitudes are deduced in Sec. IV. We present our calculations and discussions in Sec. V. Finally, a summary is given in Sec. VI.

II. MESON SPECTROSCOPY

A. Harmonic oscillator states

For a heavy-light $\bar{Q}q$ system consisting of light quark 1 and heavy quark 2 with masses m_1 and m_2, respectively, its eigenstates are conventionally generated by a harmonic oscillator potential

$$\mathcal{H} = \frac{1}{2m_1}\mathbf{p}_1^2 + \frac{1}{2m_2}\mathbf{p}_2^2 + \frac{3}{2}K(\mathbf{r}_1 - \mathbf{r}_2)^2, \tag{1}$$

where vectors $\mathbf{r}_j$ and $\mathbf{p}_j$ are the coordinate and momentum for the jth quark in the meson rest frame, and K describes the oscillator potential strength which is independent of the flavor quantum number. One defines the Jacobi coordinates to eliminate the c.m. variables:

$$\mathbf{r} = \mathbf{r}_1 - \mathbf{r}_2, \tag{2}$$

$$\mathbf{R}_{\text{c.m.}} = \frac{m_1\mathbf{r}_1 + m_2\mathbf{r}_2}{m_1 + m_2}. \tag{3}$$

With the above relations (2) and (3), the oscillator Hamiltonian (1) is reduced to

$$\mathcal{H} = \frac{P_{\text{c.m.}}^2}{2M} + \frac{1}{2\mu}\mathbf{p}^2 + \frac{3}{2}Kr^2, \tag{4}$$

where

$$\mathbf{p} = \mu\dot{\mathbf{r}}, \qquad \mathbf{P}_{\text{c.m.}} = M\dot{\mathbf{R}}_{\text{c.m.}}, \tag{5}$$

with

$$M = m_1 + m_2, \qquad \mu = \frac{m_1 m_2}{m_1 + m_2}. \tag{6}$$

From Eqs. (2), (3), and (5), the coordinate $\mathbf{r}_j$ can be expressed as functions of the Jacobi coordinate $\mathbf{r}$,

$$\mathbf{r}_1 = \mathbf{R}_{\text{c.m.}} + \frac{\mu}{m_1}\mathbf{r}, \tag{7}$$

$$\mathbf{r}_2 = \mathbf{R}_{\text{c.m.}} - \frac{\mu}{m_2}\mathbf{r}, \tag{8}$$

and the momentum $\mathbf{p}_j$ is given by

$$\mathbf{p}_1 = \frac{m_1}{M}\mathbf{P}_{\text{c.m.}} + \mathbf{p}, \tag{9}$$

$$\mathbf{p}_2 = \frac{m_2}{M}\mathbf{P}_{\text{c.m.}} - \mathbf{p}. \tag{10}$$

Using standard notation, the principal quantum numbers of the oscillator are $N = (2n + l)$, the energy of a state is given by

$$E_N = (N + \tfrac{3}{2})\omega, \tag{11}$$

and the frequency of the oscillator is

$$\omega = (3K/\mu)^{1/2}. \tag{12}$$

In the quark model the useful oscillator parameter is defined by

$$\alpha^2 = \mu\omega = \sqrt{\frac{2m_2}{m_1 + m_2}}\beta^2, \tag{13}$$

where β is the often used harmonic oscillator parameter with a universal value $\beta = 0.4$ GeV. Then, the wave function of an oscillator is given by

$$\psi_{lm}^n = R_{nl}Y_{lm}. \tag{14}$$

B. Spin wave functions

The usual spin wave functions are adopted. For the spin-0 state, it is

$$\chi^0 = \frac{1}{\sqrt{2}}(\uparrow\downarrow - \downarrow\uparrow), \tag{15}$$

and for the spin-1 states, the wave functions are

$$\chi_1^1 = \uparrow\uparrow, \qquad \chi_{-1}^1 = \downarrow\downarrow, \qquad \chi_0^1 = \frac{1}{\sqrt{2}}(\uparrow\downarrow + \downarrow\uparrow). \tag{16}$$

We take the heavy-quark infinite mass limit as an approximation to construct the total wave function without flavor symmetry. All the wave functions up to $1D$ states are listed in Table I.

TABLE I. The total wave function for the heavy-light mesons, denoted by $|n^{2S+1}L_J\rangle$. The Clebsch-Gordan series for the spin and angular-momentum addition $|n^{2S+1}L_J\rangle = \sum_{m+S_z=J_z}\langle Lm, SS_z|JJ_z\rangle\psi^n_{Lm}\chi_{S_z}\Phi$ has been omitted, where Φ is the flavor wave function.

$\|n^{2S+1}L_J\rangle$	J^P	Wave function
$1\ {}^1S_0$	0^-	$\psi^0_{00}\chi^0\Phi$
$1\ {}^3S_1$	1^-	$\psi^0_{00}\chi^1_{S_z}\Phi$
$1\ {}^1P_1$	1^+	$\psi^0_{1m}\chi^0\Phi$
$1\ {}^3P_0$	0^+	$\psi^0_{1m}\chi^1_{S_z}\Phi$
$1\ {}^3P_1$	1^+	$\psi^0_{1m}\chi^1_{S_z}\Phi$
$1\ {}^3P_2$	2^+	$\psi^0_{1m}\chi^1_{S_z}\Phi$
$2\ {}^1S_0$	0^-	$\psi^1_{00}\chi^0\Phi$
$2\ {}^3S_1$	1^-	$\psi^1_{00}\chi^1_{S_z}\Phi$
$1\ {}^1D_2$	2^-	$\psi^0_{2m}\chi^0\Phi$
$1\ {}^3D_1$	1^-	$\psi^0_{2m}\chi^1_{S_z}\Phi$
$1\ {}^3D_2$	2^-	$\psi^0_{2m}\chi^1_{S_z}\Phi$
$1\ {}^3D_3$	3^-	$\psi^0_{2m}\chi^1_{S_z}\Phi$

III. THE QUARK-MESON COUPLINGS

In the chiral quark model, the low-energy quark-meson interactions are described by the effective Lagrangian [67,69]

$$\mathcal{L} = \bar{\psi}[\gamma_\mu(i\partial^\mu + V^\mu + \gamma_5 A^\mu) - m]\psi + \cdots, \quad (17)$$

where V^μ and A^μ correspond to vector and axial currents, respectively. They are given by

$$\begin{aligned} V^\mu &= \frac{1}{2}(\xi\partial^\mu\xi^\dagger + \xi^\dagger\partial^\mu\xi), \\ A^\mu &= \frac{1}{2i}(\xi\partial^\mu\xi^\dagger - \xi^\dagger\partial^\mu\xi), \end{aligned} \quad (18)$$

with $\xi = \exp(i\phi_m/f_m)$, where f_m is the meson decay constant. For the $SU(3)$ case, the pseudoscalar-meson octet ϕ_m can be expressed as

$$\phi_m = \begin{pmatrix} \frac{1}{\sqrt{2}}\pi^0 + \frac{1}{\sqrt{6}}\eta & \pi^+ & K^+ \\ \pi^- & -\frac{1}{\sqrt{2}}\pi^0 + \frac{1}{\sqrt{6}}\eta & K^0 \\ K^- & \bar{K}^0 & -\sqrt{\frac{2}{3}}\eta \end{pmatrix}, \quad (19)$$

and the quark field ψ is given by

$$\psi = \begin{pmatrix} \psi(u) \\ \psi(d) \\ \psi(s) \end{pmatrix}. \quad (20)$$

From the leading order of the Lagrangian [see Eq. (17)], we obtain the standard quark-meson pseudovector coupling at tree level

$$H_m = \sum_j \frac{1}{f_m} I_j \bar{\psi}_j \gamma^j_\mu \gamma^j_5 \psi_j \partial^\mu \phi_m, \quad (21)$$

where ψ_j represents the jth quark field in a hadron, and I_j is the isospin operator to be given later.

In the quark model, the nonrelativistic form of Eq. (21) is written as [67,69,72]

$$\begin{aligned} H^{nr}_m = \sum_j \Big\{ &\frac{\omega_m}{E_f + M_f}\boldsymbol{\sigma}_j\cdot\mathbf{P}_f + \frac{\omega_m}{E_i + M_i}\boldsymbol{\sigma}_j\cdot\mathbf{P}_i - \boldsymbol{\sigma}_j\cdot\mathbf{q} \\ &+ \frac{\omega_m}{2\mu_q}\boldsymbol{\sigma}_j\cdot\mathbf{p}'_j\Big\} I_j\varphi_m, \end{aligned} \quad (22)$$

where $\boldsymbol{\sigma}_j$ corresponds to the Pauli spin vector of the jth quark in a hadron. μ_q is a reduced mass given by $1/\mu_q = 1/m_j + 1/m'_j$, where m_j and m'_j stand for the masses of the jth quark in the initial and final hadrons, respectively. For emitting a meson, we have $\varphi_m = \exp(-i\mathbf{q}\cdot\mathbf{r}_j)$, and for absorbing a meson we have $\varphi_m = \exp(i\mathbf{q}\cdot\mathbf{r}_j)$. In the above nonrelativistic expansions, $\mathbf{p}'_j = \mathbf{p}_j - \frac{m_j}{M}\mathbf{P}_{\text{c.m.}}$ is the internal momentum for the jth quark in the initial meson rest frame. ω_m and $\mathbf{q}$ are the energy and three-vector momentum of the light meson, respectively. The isospin operator I_j in Eq. (21) is expressed as

$$I_j = \begin{cases} a^\dagger_j(u)a_j(s) & \text{for } K^+, \\ a^\dagger_j(s)a_j(u) & \text{for } K^-, \\ a^\dagger_j(d)a_j(s) & \text{for } K^0, \\ a^\dagger_j(s)a_j(d) & \text{for } \bar{K}^0, \\ a^\dagger_j(u)a_j(d) & \text{for } \pi^-, \\ a^\dagger_j(d)a_j(u) & \text{for } \pi^+, \\ \frac{1}{\sqrt{2}}[a^\dagger_j(u)a_j(u) - a^\dagger_j(d)a_j(d)] & \text{for } \pi^0, \\ \cos\theta\frac{1}{\sqrt{2}}[a^\dagger_j(u)a_j(u) + a^\dagger_j(d)a_j(d)] - \sin\theta a^\dagger_j(s)a_j(s) & \text{for } \eta, \end{cases} \quad (23)$$

where $a^\dagger_j(u, d, s)$ and $a_j(u, d, s)$ are the creation and annihilation operators for the u, d, and s quarks. Generally, θ ranges from $\simeq 32^\circ \sim 43^\circ$ depending on the quadratic or line mass relation applied [74]. In our convention, $\theta = 45^\circ$ corresponds to the mixing scheme of Ref. [19]. We applied the same value in order to compare with Ref. [19]. However, we note in advance that within the commonly accepted range of θ, our results do not show great sensi-

TABLE II. The spin factors used in this work.

$$
\begin{aligned}
g^z_{10} &= \langle \chi^0 | \sigma_{1z} | \chi^1_0 \rangle = 1 \\
g^+_{10} &= \langle \chi^0 | \sigma^+_1 | \chi^1_{-1} \rangle = \sqrt{\tfrac{1}{2}} \\
g^-_{10} &= \langle \chi^0 | \sigma^-_1 | \chi^1_1 \rangle = -\sqrt{\tfrac{1}{2}} \\
g^z_{01} &= \langle \chi^1_0 | \sigma_{1z} | \chi^0 \rangle = 1 \\
g^+_{01} &= \langle \chi^1_1 | \sigma^+_1 | \chi^0 \rangle = -\sqrt{\tfrac{1}{2}} \\
g^z_{11} &= \langle \chi^1_1 | \sigma_{1z} | \chi^1_1 \rangle = 1 \\
g^+_{11} &= \langle \chi^1_1 | \sigma^+_1 | \chi^1_0 \rangle = \sqrt{\tfrac{1}{2}}
\end{aligned}
$$

tivities due to the relatively large uncertainties of the present experimental data.

IV. STRONG DECAYS

For a heavy-light meson $\bar{Q}q$, because the pseudoscalar mesons $\mathbb{P}$ only couple with the light quarks, the strong decay amplitudes for the process $\mathbb{M}_i \to \mathbb{M}_f \mathbb{P}$ can be written as

$$
\begin{aligned}
\mathcal{M}(\mathbb{M}_i \to \mathbb{M}_f \mathbb{P}) = \langle \mathbb{M}_f | \{ \mathcal{G} \boldsymbol{\sigma}_1 \cdot \mathbf{q} + h \boldsymbol{\sigma}_1 \cdot \mathbf{p}'_1 \} \\
\times I_1 e^{-i\mathbf{q}\cdot\mathbf{r}_1} | \mathbb{M}_i \rangle,
\end{aligned} \tag{24}
$$

with

$$
\mathcal{G} \equiv -\left(\frac{\omega_m}{E_f + M_f} + 1 \right), \qquad h \equiv \frac{\omega_m}{2\mu_q}. \tag{25}
$$

$\mathbb{M}_i$ and $\mathbb{M}_f$ are the initial and final meson wave functions, and they are listed in Table I. In the initial meson rest frame the energies and momenta of the initial mesons $\mathbb{M}_i$ are denoted by $(E_i, \mathbf{P}_i)$, while those of the final state mesons $\mathbb{M}_f$ and the emitted pseudoscalar mesons $\mathbb{P}$ are denoted by $(E_f, \mathbf{P}_f)$ and $(\omega_m, \mathbf{q})$. Note that $\mathbf{P}_i = 0$ and $\mathbf{P}_f = -\mathbf{q}$.

The form of Eq. (24) is similar to that in Refs. [21,22], except that the factors $\mathcal{G}$ and h in this work have explicit dependence on the energies of final hadrons. In the calculations, we select $\mathbf{q} = q\hat{z}$; namely, the meson moves along the z axial. The spin factors can then be worked out, and we list them in Table II. Finally, we can work out the decay amplitudes for various processes, $\mathbb{M} \to |1^1S_0\rangle\mathbb{P}$, $\mathbb{M} \to |1^3S_1\rangle\mathbb{P}$, $\mathbb{M} \to |1^3P_0\rangle\mathbb{P}$, $\mathbb{M} \to |1^1P_1\rangle\mathbb{P}$, and $\mathbb{M} \to |1^3P_1\rangle\mathbb{P}$, which are listed in Tables III, IV, V, VI, and VII, respectively.

Some analytical features can be learned here. Table III shows that the decays of 1^1P_1, 1^3P_1, 2^1S_0, 1^1D_2, and 1^3D_2 into $|1^1S_0\rangle\mathbb{P}$ are forbidden by parity conservation. The

TABLE III. The decay amplitudes for $|n^{2S+1}L_J\rangle \to |1^1S_0\rangle\mathbb{P}$. g_I is an isospin factor which is defined by $g_I = \langle \phi_\Sigma | I_1 | \phi_\Lambda \rangle$. In the Table III, IV, V, VI, and VII, the overall factor $F(q') = \exp(-\frac{q'^2}{4\alpha^2})$, which plays the role of the decay form factor, is omitted for simplicity, where $q' = (\mu/m_1)q$. In the tables, we have defined $\mathcal{R} \equiv (\mathcal{G}q - \frac{1}{2}hq')$. Various spin factors used in this work are listed in Table II.

Initial state	Amplitude
$1^3S_1(1^-)$	$g_I g^z_{10} \mathcal{R}$
$1^1P_1(1^+)$	Forbidden
$1^3P_0(0^+)$	$i\frac{1}{\sqrt{6}} g_I g^z_{10} \mathcal{R} \frac{q'}{\alpha} + i\frac{1}{\sqrt{6}} g_I (\sqrt{2} g^+_{10} + g^z_{10}) h\alpha$
$1^3P_1(1^+)$	Forbidden
$1^3P_2(2^+)$	$i\frac{1}{\sqrt{3}} g_I g^z_{10} \mathcal{R} \frac{q'}{\alpha}$
$2^1S_0(0^-)$	Forbidden
$2^3S_1(1^-)$	$\frac{1}{\sqrt{24}} g_I g^z_{10} \mathcal{R} (\frac{q'}{\alpha})^2 + \sqrt{\frac{1}{6}} g_I g^z_{10} h q'$
$1^1D_2(2^-)$	Forbidden
$1^3D_1(1^-)$	$\frac{1}{\sqrt{30}} g_I g^z_{10} \mathcal{R} (\frac{q'}{\alpha})^2 + \sqrt{\frac{3}{5}} g_I g^+_{10} h q'$
$1^3D_2(2^-)$	Forbidden
$1^3D_3(3^-)$	$-\frac{1}{\sqrt{20}} g_I g^z_{10} \mathcal{R} (\frac{q'}{\alpha})^2$

TABLE IV. The decay amplitudes for $|n^{2S+1}L_J\rangle \to |1^3S_1\rangle\mathbb{P}$.

$\lvert n^{2S+1}L_J\rangle$	J_z	Amplitude
$1^1P_1(1^+)$	± 1	$i g_I g^+_{01} h\alpha$
	0	$-i\frac{1}{\sqrt{2}} g_I g^z_{01} \mathcal{R} \frac{q'}{\alpha} - i\frac{1}{\sqrt{2}} g_I g^z_{01} h\alpha$
$1^3P_0(0^+)$		Forbidden
$1^3P_1(1^+)$	± 1	$i\frac{1}{2} g_I g^z_{11} \mathcal{R} \frac{q'}{\alpha} + i\frac{1}{2} g_I (g^z_{11} + \sqrt{2} g^+_{11}) h\alpha$
	0	$\sqrt{2} g_I g^+_{11} h\alpha$
$1^3P_2(2^+)$	± 1	$-i\frac{1}{2} g_I g^z_{11} \mathcal{R} \frac{q'}{\alpha}$
	0	0
$2^1S_0(0^-)$	0	$\frac{1}{\sqrt{24}} g_I g^z_{10} \mathcal{R} (\frac{q'}{\alpha})^2 + \sqrt{\frac{1}{6}} g_I g^z_{10} h q'$
$2^3S_1(1^-)$	± 1	$\pm\{\frac{1}{\sqrt{24}} g_I g^z_{11} \mathcal{R} (\frac{q'}{\alpha})^2 F + \sqrt{\frac{1}{6}} g_I g^z_{11} h q'\}$
	0	0
$1^1D_2(2^-)$	± 1	$\frac{1}{\sqrt{2}} g^+_{01} g_I h q'$
	0	$-\sqrt{\frac{1}{12}} g_I g^z_{01} \mathcal{R} (\frac{q'}{\alpha})^2 - \sqrt{\frac{1}{3}} g_I g^+_{01} h q'$
$1^3D_1(1^-)$	± 1	$\mp[\sqrt{\frac{1}{120}} g_I g^z_{11} \mathcal{R} (\frac{q'}{\alpha})^2 + \sqrt{\frac{5}{12}} g_I g^+_{11} h q']$
	0	0
$1^3D_2(2^-)$	± 1	$\sqrt{\frac{1}{24}} g_I g^z_{10} \mathcal{R} (\frac{q'}{\alpha})^2 + \sqrt{\frac{3}{4}} g_I g^+_{11} h q'$
	0	$g^+_{11} g_I h q'$
$1^3D_3(3^-)$	± 1	$\mp\sqrt{\frac{1}{30}} g_I g^z_{11} \mathcal{R} (\frac{q'}{\alpha})^2$
	0	0

TABLE V. The decay amplitudes for $|n^{2S+1}L_J\rangle \to |1^3P_0\rangle\mathbb{P}$, where we have defined $\mathcal{W} \equiv \mathcal{G}q(-1 + \frac{q'^2}{4\alpha^2})$, $\mathcal{S} \equiv h\alpha(1 - \frac{q'^2}{2\alpha^2})$.

$\lvert n^{2S+1}L_J\rangle$	J_z	Amplitude
$2^1S_0(0^-)$	0	$i\frac{1}{3} g_I g^z_{01} \mathcal{W} \frac{q'}{\alpha} - i\frac{1}{3} g_I g^z_{01} h\alpha \mathcal{A}$
$2^3S_1(1^-)$		Forbidden
	0	$i\frac{\sqrt{2}}{3} g_I g^z_{01} \mathcal{W} \frac{q'}{\alpha} + i\frac{\sqrt{2}}{3} g_I g^z_{01} h\alpha \mathcal{A}$
$1^1D_2(2^-)$	± 1	0
	± 2	$-i\frac{\sqrt{2}}{3} g_I g^+_{01} h\alpha$
$1^3D_1(1^-)$		Forbidden
	0	$-i\frac{\sqrt{6}}{3} g^+_{11} g_I \mathcal{S}$
$1^3D_2(2^-)$	± 1	0
	± 2	$-i\frac{2}{3} g^+_{11} g_I h\alpha F - i\frac{\sqrt{2}}{6} g^z_{11} g_I \mathcal{S}$
$1^3D_3(3^-)$	± 2	$-i\frac{\sqrt{2}}{3} g^+_{11} g_I h\alpha F + i\frac{1}{3} g^z_{11} g_I \mathcal{S}$

TABLE VI. The decay amplitudes for $|n^{2S+1}L_J\rangle \to |1^1P_1\rangle\mathbb{P}$.

$\|n^{2S+1}L_J\rangle$	(J_z^f, J_z^i)	Amplitude
$2^1S_0(0^-)$		Forbidden
$2^3S_1(1^-)$	$\pm(1,-1)$	$-i\sqrt{\frac{2}{3}}g_I g^+_{10} h\alpha(1+\frac{q'^2}{4\alpha^2})$
	(0,0)	$-i\frac{1}{\sqrt{3}}g_I g^z_{10}\mathcal{W}\frac{q'}{\alpha} + i\frac{1}{\sqrt{3}}g_I g^z_{10} h\alpha\mathcal{A}$
$1^1D_2(2^-)$		Forbidden
$1^3D_1(1^-)$	$\pm(1,-1)$	$-i\sqrt{\frac{3}{20}}g_I g^z_{10}\mathcal{G}q\frac{q'}{\alpha} - i\sqrt{\frac{1}{30}}g_I g^+_{10}\mathcal{S}$
	(0,0)	$-i\sqrt{\frac{4}{15}}g_I g^z_{10}\mathcal{W}\frac{q'}{\alpha} + i\sqrt{\frac{4}{15}}g_I g^z_{10} h\alpha\mathcal{A}$
$1^3D_2(2^-)$	$\pm(1,-1)$	$-i\frac{1}{\sqrt{12}}g_I g^z_{10}\mathcal{R}\frac{q'}{\alpha} + i\frac{1}{\sqrt{24}}g_I g^+_{10} hq'\frac{q'}{\alpha}$
$1^3D_3(3^-)$	$\pm(1,-1)$	$-i\sqrt{\frac{1}{30}}(\sqrt{2}g^z_{10} - g^+_{10})g_I hq'\frac{q'}{\alpha}$
	(0,0)	$i\sqrt{\frac{1}{5}}g_I[g^z_{10}\mathcal{W}\frac{q'}{\alpha} - \sqrt{2}g^z_{10} h\alpha\mathcal{A} + 2g^+_{10}\mathcal{S}]$

decay amplitudes for 1^3S_1, 1^3P_2, and $1^3D_3 \to |1^1S_0\rangle\mathbb{P}$ are proportional to $\mathcal{R}$ (i.e. proportional to q), $\mathcal{R}q'/\alpha$, and $\mathcal{R}(q/\alpha)^2$, respectively. This is crucial for understanding the small branching ratios for $D^*(2007) \to D\pi$ as we will see later.

In contrast, the decay amplitude for $1^3P_0 \to |1^1S_0\rangle\mathbb{P}$ has two terms. One is proportional to $\mathcal{R}q'/\alpha$, while the other is proportional to α. Similarly, the decay amplitudes for $2^3S_1 \to |^1S_0\rangle\mathbb{P}$ and $2^3D_1 \to |1^1S_0\rangle\mathbb{P}$ also have two terms of which one is proportional to $\mathcal{R}(q'/\alpha)^2$, and the other to q'. This feature will have certain implications for their branching ratio rates into different $|1^1S_0\rangle\mathbb{P}$ states.

Table IV shows that decays of 1^3P_0 into $|1^1S_0\rangle\mathbb{P}$ are forbidden. Among those three helicity amplitudes $\mathcal{M}_\pm$ and $\mathcal{M}_0$, the longitudinal one $\mathcal{M}_0$ vanishes for 1^3P_2, 2^3S_1, 1^3D_1, and 1^3D_3 into $|1^1S_0\rangle\mathbb{P}$.

From Tables V, VI, and VII, we can see that the decays of 2^3S_1 and 1^3D_1 into $|1^3P_0\rangle\mathbb{P}$, 2^1S_0 and 1^1D_2 into $|1^1P_1\rangle\mathbb{P}$, and 2^1S_0 into $|1^1P_1\rangle\mathbb{P}$ are forbidden parity conservation. These selection rules are useful for the state classifications.

TABLE VII. The decay amplitudes for $|n^{2S+1}L_J\rangle \to |1^3P_1\rangle\mathbb{P}$.

$\|n^{2S+1}L_J\rangle$	(J_z^f, J_z^i)	Amplitude
$2^1S_0(0^-)$		Forbidden
$2^3S_1(1^-)$	$\pm(1,-1)$	$-i\frac{1}{\sqrt{3}}g_I g^+_{11} h\alpha(1+\frac{q'^2}{4\alpha^2})$
	$\pm(1,1)$	$i\frac{1}{\sqrt{6}}g_I g^z_{11}\mathcal{W}\frac{q'}{\alpha} - i\frac{1}{\sqrt{6}}g_I g^z_{11} h\alpha\mathcal{A}$
	$\pm(0,2)$	$\pm i g^+_{01} h\alpha$
$1^1D_2(2^-)$	$\pm(1,1)$	$\pm i\frac{1}{\sqrt{2}}g^+_{01}\mathcal{S}$
	$\pm(1,-1)$	$\pm i\frac{1}{2}g_I g^z_{01}(\mathcal{R}\frac{q'}{\alpha} + h\alpha)$
$1^3D_1(1^-)$	$\pm(1,-1)$	$-i\sqrt{\frac{1}{60}}g_I g^+_{11} h\alpha(1+\frac{q'^2}{2\alpha^2})$
	$\pm(1,1)$	$-i\sqrt{\frac{1}{30}}g_I g^z_{11}(\mathcal{W}\frac{q'}{\alpha} - h\alpha\mathcal{A} - \frac{3}{2}\mathcal{S})$
	$\pm(0,2)$	$\pm i\frac{1}{\sqrt{12}}g_I g^z_{11}(\mathcal{R}\frac{q'}{\alpha} + 3h\alpha)$
$1^3D_2(2^-)$	$\pm(1,-1)$	$\pm[-i\sqrt{\frac{1}{3}}g_I g^z_{11} h\alpha - i\sqrt{\frac{1}{12}}g^+_{11}\mathcal{S}]$
	$\pm(1,1)$	$\pm i\sqrt{\frac{1}{6}}g_I g^z_{11}(\mathcal{W}\frac{q'}{\alpha} - h\alpha\mathcal{A} - \frac{1}{2}\mathcal{S})$
	$\pm(0,2)$	$i\frac{1}{\sqrt{6}}g_I g^z_{11}\mathcal{R}\frac{q'}{\alpha}$
$1^3D_3(3^-)$	$\pm(1,-1)$	$-i\sqrt{\frac{1}{60}}g_I g^+_{11} hq'\frac{q'}{\alpha}$
	$\pm(1,1)$	$-i\sqrt{\frac{2}{15}}g_I g^z_{11}[\mathcal{W}\frac{q'}{\alpha} - h\alpha\mathcal{A} + \mathcal{S}]$

V. CALCULATIONS AND ANALYSIS

With the transition amplitudes, one can calculate the partial decay width with

$$\Gamma = \left(\frac{\delta}{f_m}\right)^2 \frac{(E_f + M_f)|\mathbf{q}|}{4\pi M_i(2J_i+1)} \sum_{J_{iz},J_{fz}} |\mathcal{M}_{J_{iz},J_{fz}}|^2, \tag{26}$$

where J_{iz} and J_{fz} stand for the third components of the total angular momenta of the initial and final heavy-light mesons, respectively. δ as a global parameter accounts for the strength of the quark-meson couplings. In the heavy-light meson transitions, the flavor symmetry does not hold anymore. Treating the light pseudoscalar meson as a chiral field while treating the heavy-light mesons as constituting a quark system is an approximation. This will bring uncertainties to coupling vertices and form factors. Parameter δ is introduced to take into account such an effect. It has been determined in our previous study of the strong decays of the charmed baryons [73]. Here, we fix its value as the same as that in Ref. [73], i.e. $\delta = 0.557$.

In the calculation, the standard parameters in the quark model are adopted. For the u, d, s, c, and b constituent quark masses we set $m_u = m_d = 350$ MeV, $m_s = 550$ MeV, $m_c = 1700$ MeV, and $m_b = 5100$ MeV, respectively. The decay constants for π, K, η, and D mesons, $f_\pi = 132$ MeV, $f_K = f_\eta = 160$ MeV, and $f_D = 226$ MeV, are used. For the masses of all the heavy-light mesons the Particle Data Group (PDG) values are adopted in the calculations [74].

To partly remedy the inadequacy of the nonrelativistic wave function as the relative momentum q increases, a commonly used Lorentz boost factor is introduced into the decay amplitudes [66,71,72],

$$\mathcal{M}(q) \to \gamma_f \mathcal{M}(\gamma_f q), \tag{27}$$

where $\gamma_f = M_f/E_f$. In most decays, the three momenta carried by the final state mesons are relatively small, which means the nonrelativistic prescription is reasonable and corrections from the Lorentz boost are not drastic.

A. Strong decays of 1S states

Because of isospin violation, D^{*+} is about 3 MeV heavier than the neutral D^{*0} [74]. This small difference leads to a kinematic forbiddance of $D^{*0} \to D^+\pi^-$, while $D^{*+} \to D^0\pi^+$ and $D^+\pi^0$ are allowed, but with a strong kinematic suppression. Nevertheless, it shows in Table III that the decay amplitudes of $1S$ states are proportional to the final state momentum q. For the decays of $D^{*0} \to D^0\pi^0$, $D^{*+} \to D^0\pi^+$, and $D^+\pi^0$ of which the decay thresholds are close to the D^* masses, it leads to further dynamic suppressions to the partial decay widths. As shown in

TABLE VIII. Predictions of the strong decay widths (in MeV) for the heavy-light mesons. For comparison, the experimental data and some other model predictions are listed.

	Notation	Channel	Γ (this work)	Γ [19]	Γ [20]	Γ [32]	Γ [30,31]	Γ [26]	$\Gamma_{\rm exp}$
$D^*(2007)^0$	$(1^3S_1)1^-$	$D^0\pi^0$	58 keV	16 keV		39 keV			<2.1 MeV
$D^*(2010)^+$		$D^0\pi^+$	77 keV	25 keV		60 keV			64 ± 15 keV
		$D^+\pi^0$	35 keV	11 keV		27 keV			29 ± 7 keV
$D_0^*(2352)$	$(1^3P_0)0^+$	$D\pi$	248		277				261 ± 50
$D_0^*(2403)$			266	283					283 ± 58
$D_1(2420)$	$(1^1P_1)1^+$	$D^*\pi$	84						
	$(P_1)1^+$		21.6	22	25				25 ± 6
$D_1'(2430)$	$(1^3P_1)1^+$	$D^*\pi$	152						
	$(P_1')1^+$		220	272	244				384 ± 117
$D_2^*(2460)^0$	$(1^3P_2)2^+$	$D\pi$	39	35	37		13.7		
		$D^*\pi$	19	20	18		6.1		
		$D\eta$	0.1	0.08					
		Total	59	55	55		20		43 ± 4
$D_{s1}(2536)$	$(1^1P_1)1^+$	D^*K	59						
	$(P_1)1^+$		0.35	0.8	0.34				<2.3
$D_{s2}^*(2573)$	$(1^3P_2)2^+$	DK	16	27	20				
		D^*K	1	3.1	1				
		$D_s\eta$	0.4	0.2					
		Total	17	30	21				15^{+5}_{-4}
$D_{sJ}^*(2860)$	$(1^3D_3)3^-$	DK	27						
		D^*K	11						
		$D_s\eta$	3						
		$D_s^*\eta$	0.3						
		DK^*	0.4						
		Total	42						48 ± 17
$B_0^*(5730)$	$(^3P_0)0^+$	$B\pi$	272			141	250		
$B_1(5725)$	$(P_1)1^+$	$B^*\pi$	30			20			20 ± 12
	$(1^3P_1)1^+$	$B^*\pi$	153						
$B_1'(5732)$	$(P_1')1^+$	$B^*\pi$	219			139	250		128 ± 18
$B_2^*(5740)$	$(1^3P_2)2^+$	$B\pi$	25			15	3.9		
		$B^*\pi$	22			14	3.4		
		Total	47			29	7.3	16 ± 6	22^{+7}_{-6}
$B_{s0}^*(5800)$	$(^3P_0)0^+$	BK	227						
$B_{s1}(5830)$	$(P_1)1^+$	B^*K	0.4 ∼ 1					3 ± 1	1
$B_{s1}'(5830)$	$(P_1')1^+$	B^*K	149						
$B_{s2}^*(5839)$	$(1^3P_2)2^+$	BK	2						
		B^*K	0.12						
		Total	2					7 ± 3	1

Table VIII, our calculations are in remarkable agreement with the experimental data. Since q is small, the form factor corrections from the quark model are negligibly small. One would expect that the ratio $\Gamma(D^0\pi^+)/\Gamma(D^+\pi^0) \simeq 2$ is then dominated by the isospin factor g_I, which agrees well with the prediction in Ref. [19].

B. Strong decays of 1P states

In the LS coupling scheme, there are four $1P$ states: $^3P_0$, $^3P_1$, $^3P_2$, and $^1P_1$. For $^3P_0$, its transition to $|1^3S_1\rangle\mathbb{P}$ is forbidden. States of $^1P_1$ and $^3P_1$ can couple into $|1^3S_1\rangle\mathbb{P}$, but not $|1^1S_0\rangle\mathbb{P}$. In contrast, $^3P_2$ can be coupled to both $|1^3S_1\rangle\mathbb{P}$ and $|1^1S_0\rangle\mathbb{P}$. In the decay amplitudes of $^3P_0$, $^1P_1$, and $^3P_1$, the term $h\alpha F$ dominates the partial decay widths, and usually their decay widths are much broader than that of $^3P_2$. Between the amplitudes of the $^1P_1$ and $^3P_1$ decays, we approximately have

$$\mathcal{M}(^1P_1 \to |1^3S_1\rangle\mathbb{P})_{J_z} \simeq \frac{1}{\sqrt{2}}\mathcal{M}(^3P_1 \to |1^3S_1\rangle\mathbb{P})_{J_z}, \quad (28)$$

since the term $\mathcal{R}\frac{q'}{\alpha}F$ is negligible when the decay channel threshold is close to the initial meson mass. As a consequence, the decay widths of the $^1P_1$ states are narrower than those of $^3P_1$.

1. $^3P_0$ states

$D_0^*(2400)$ is listed by the PDG [74] as a broad $^3P_0$ state. Its mass values from Belle [75] and the FOCUS Collaboration [76] are quite different though the FOCUS result is consistent with the potential quark model prediction of 2403 MeV [21]. In experiments, only the $D\pi$ channel is observed since the other channels are forbidden. The term $h\alpha F$ in the amplitude, which is in proportion to the oscillator parameter α, accounts for the broad decay width. By applying the PDG averaged mass 2352 MeV and the FOCUS value 2403 MeV, its partial decay widths into $D\pi$ are calculated and presented in Table VIII. They are in good agreement with the data [74,76].

In the B meson sector, B_0^* and B_{s0}^*, as the $^3P_0$ states, have not been confirmed in any experiments. The predicted mass for B_0^* and B_{s0}^* mesons is about 5730 MeV and 5800 MeV, respectively [47]. Their strong decays only open to $B\pi$ or BK. Applying the theory-predicted masses, we obtain broad decay widths for both states, i.e. $\Gamma(B_0^*) = 272$ MeV and $\Gamma(B_{s0}^*) = 227$ MeV, respectively. Our prediction of $\Gamma(B_0^*) = 272$ MeV is compatible with the QCD sum rules prediction $\Gamma(B_0^*) \simeq 250$ MeV [30]. Such broad widths may explain why they have not yet been identified in experiments.

2. $^3P_2$ states

In the PDG, the decay width of $D_2^*(2460)^0$ is $\Gamma = 43 \pm 4$ MeV and that of $D_2^*(2460)^\pm$ is $\Gamma = 29 \pm 5$ MeV. Since there is no obvious dynamic reason for such a significant difference, it may simply be due to experimental uncertainties. Our prediction $\Gamma = 59$ MeV as a sum of the partial widths of $D\pi$, $D^*\pi$, and $D\eta$ is comparable with the data. Nevertheless, the partial width ratio

$$R \equiv \frac{\Gamma(D\pi)}{\Gamma(D^*\pi)} \simeq 2.1 \tag{29}$$

obtained here is also in good agreement with the data $R \simeq 2.3 \pm 0.6$ [74].

$D_{s2}^*(2573)$ is assigned to be a $^3P_2$ state. Its total width is $\Gamma_{\rm exp} = 15^{+5}_{-4}$, and the width ratio between D^*K and DK is $R \equiv \Gamma(D^*K)/\Gamma(DK) < 0.33$ [74]. Our predictions for the total width and ratio R are

$$\Gamma = 17 \text{ MeV}, \tag{30}$$

$$R \equiv \frac{\Gamma(D^*K)}{\Gamma(DK)} \simeq 6\%, \tag{31}$$

which are consistent with the data.

Notice that the width of D^*K, $\sim$1 MeV, is 1 order of magnitude smaller than that of DK. Apart from the kinematic phase space suppression, its transition amplitude also suffers dynamic suppressions since it is proportional to $\mathcal{R}q'/\alpha$. This explains its absence in experiments. Although the decay channel $D\eta/D_s\eta$ is also opened for $D_2^*(2460)/D_{s2}^*(2573)$, its partial width is negligibly small, i.e. <1 MeV.

In the B meson sector, a candidate of the $^3P_2$ state is from the CDF Collaboration with mass [8]

$$M(B_2^*) = 5740 \pm 2 \pm 1 \text{ MeV}. \tag{32}$$

The D0 Collaboration also observed the same state with slightly different masses, $M(B_2^*) = 5746.8 \pm 2.4 \pm 1.7$ MeV [9]. By assigning B_2^* as a $^3P_2$ state, the predicted total width as a sum of $B\pi$ and $B^*\pi$ is

$$\Gamma(B_2^*) \simeq 47 \text{ MeV}, \tag{33}$$

which is consistent with the CDF measurement $\Gamma(B_2^*)_{\rm exp} \simeq 22^{+7}_{-6}$ MeV. It shows that these two partial widths of $B\pi$ and $B^*\pi$ are comparable, and the predicted width ratio is

$$R \equiv \frac{\Gamma(B^*\pi)}{\Gamma(B^*\pi) + \Gamma(B\pi)} = 0.47. \tag{34}$$

This is also in good agreement with the recent D0 data $R = 0.475 \pm 0.095 \pm 0.069$ [9].

The CDF Collaboration also reported an observation of B_2^*'s strange analogue B_{s2}^* [10], of which the mass is

$$M(B_{s2}^*) = 5840 \pm 1 \text{ MeV}. \tag{35}$$

With this mass, we obtain its partial decay widths, $\Gamma(B^*K) = 0.12$ MeV and $\Gamma(BK) = 2$ MeV, respectively. This gives its strong decay width and width ratio between B^*K and BK:

$$\Gamma(B_{s2}^*) \simeq 2 \text{ MeV}, \qquad R \equiv \frac{\Gamma(B^*K)}{\Gamma(BK)} \simeq 6\%. \tag{36}$$

The decay width is in good agreement with the data $\Gamma(B_{s2}^*)_{\rm exp} \sim 1$ MeV [77]. It also shows that the partial width of the B^*K channel is negligibly small, and will evade from observations in experiments. But a measurement of $\Gamma(BK)$ with improved statistics should be very interesting.

3. The mixed states

The $D_1(2420)$ and $D_1'(2430)$ listed by PDG [74] correspond to a narrow and broad state, respectively. Their two body pionic decays are only seen in $D^*\pi$. If they are pure P-wave states, they should be correspondent to $^1P_1$ and $^3P_1$. The calculated decay widths by assigning them as $^1P_1$ and $^3P_1$, are listed in Table VIII. It shows that for $D_1(2420)$ as a pure $^1P_1$ state, its decay width is overestimated by about an order, while for $D_1'(2430)$ as a pure $^3P_1$ state, its decay width is underestimated by about a factor of 2. Similarly large discrepancies are also found if one simply exchanges the assignments. Thus, the pure $^1P_1$ and $^3P_1$ scenario cannot explain the nature of $D_1(2420)$ and $D_1'(2430)$.

Since the heavy-light mesons are not charge conjugation eigenstates, state mixing between spin $\mathbf{S} = 0$ and $\mathbf{S} = 1$

states with the same J^P can occur. The physical states with $J^P = 1^+$ would be given by

$$|P_1'\rangle = +\cos(\phi)|^1P_1\rangle + \sin(\phi)|^3P_1\rangle, \quad (37)$$

$$|P_1\rangle = -\sin(\phi)|^1P_1\rangle + \cos(\phi)|^3P_1\rangle. \quad (38)$$

Our present knowledge about the $D_1(2420)$ and $D_1'(2430)$ mixing is still limited. The determination of the mixing angle is correlated with quark potential, and masses of the states [22]. An analysis by Ref. [19] suggests that a mixed state dominated by S-wave decay will have a broad width, and the D-wave-dominant decay will have a narrow one. By assuming that the heavy-quark spin-orbit interaction is positive, this leads to an assignment of $D_1'(2430)$ and $D_1(2420)$ as a mixed $|P_1'\rangle$ and $|P_1\rangle$, respectively, with a negative mixing angle $\phi = -54.7°$. However, this will lead to the mass of D_1 being heavier than that of D_1', and the present experimental precision seems unable to rule out such a possibility [74]. An additional piece of information supporting such a scenario is that a positive spin-orbit interaction will lead to a heavier 2^+ state than 0^+ which indeed agrees with experiments [19].

In our calculation, we plot the pionic decay widths of the mixed states $|P_1'\rangle$ and $|P_1\rangle$ as functions of ϕ in Fig. 1. By looking for the best description of the experimental data, we determine the optimal mixing angle. It shows that with $\phi = -(55 \pm 5)°$, $D_1(2420)$, as the $|P_1\rangle$ mixed state, has a narrow decay width of $\Gamma \simeq 22$ MeV. This value agrees well with the experimental data (see Table VIII). Our prediction for the width of $D_1'(2430)$ as a $|P_1'\rangle$ broad state is $\Gamma \simeq 217$ MeV, which also agrees with the data [74]. Note that there are still large uncertainties with the

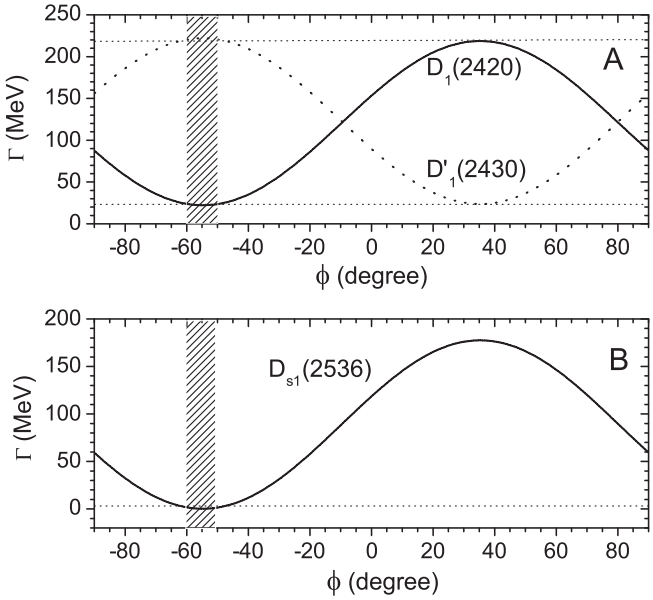

FIG. 1. The decay widths of $D_1(2420)$, $D_1'(2430)$, and $D_{s1}(2536)$ as functions of the mixing angle ϕ.

$D_1'(2430)$ measurements, and further experimental investigation is needed.

Such a mixing scenario may occur within the D_{s1} states, which leads to $D_{s1}(2460)$ and $D_{s1}(2536)$ as the mixed $|P_1'\rangle$ and $|P_1\rangle$, respectively. Note that $D_{s1}(2460)$ has a relatively light mass which is below the D^*K threshold, and also slightly below the DK threshold. Therefore, its strong decay is nearly forbidden, which makes it a narrow state. On the other hand, $D_{s1}(2536)$, as a $|P_1\rangle$ mixed state with the mixing angle $\phi = -(55 \pm 5)°$, can give a decay width consistent with the data ($\Gamma < 2.3$ MeV)

$$\Gamma(D_{s1}(2536)) \simeq 0.4 \sim 2.5 \text{ MeV}. \quad (39)$$

In contrast, if $D_{s1}(2536)$ is a pure $^1P_1$ state, its decay width will be 59 MeV, which is overestimated by a factor of 20.

We also derive the width ratio

$$R \equiv \frac{\Gamma(D^*(2007)^0K^+)}{\Gamma(D^*(2010)^+K^0)} \simeq 1.2 \sim 1.7, \quad (40)$$

which is consistent with the experimental result, $R = 1.27 \pm 0.27$. In Fig. 1(b), the change of the strong decay width $\Gamma(D_{s1}(2536))$ in terms of the mixing angle ϕ is presented by treating it as a mixed $|P_1\rangle$ state. It should be mentioned that the recent measurements of the angular decomposition of $D_{s1}(2536)^+ \to D^{*+}K_S^0$ indicate configuration mixings within $D_{s1}(2536)$ [78].

In the B meson sector, two new narrow excited B_1 and B_{s1} mesons are recently reported by CDF, with masses

$$M(B_1) = 5725 \pm 2 \pm 1 \text{ MeV}, \quad (41)$$

$$M(B_{s1}) = 5829 \pm 1 \text{ MeV}. \quad (42)$$

The D0 Collaboration also observed the same B_1 state with a slightly different mass, $M(B_1) = 5720 \pm 2.4 \pm 1.4$ MeV.

The narrowness of these two axial vector states makes them good candidates as the narrow heavy partners in the state mixing. With B_1 as a $|P_1\rangle$ state, its strong decay width to $B^*\pi$ is predicted to be

$$\Gamma(B_1) \simeq 30 \text{ MeV}. \quad (43)$$

With the strong decay widths for $B_2^* \to B\pi$ and $B^*\pi$ calculated, we obtain the strong decay width ratio

$$R \equiv \frac{\Gamma(B_1)}{\Gamma(B_1) + \Gamma(B_2^*)} = 0.34, \quad (44)$$

which is in good agreement with the recent D0 data $R = 0.477 \pm 0.069 \pm 0.062$ [9].

Note that $B_J^*(5732)$ in the PDG [74] is a broad state with $\Gamma_{\text{exp}} = 128 \pm 18$ MeV. The PDG averaged mass is 5698 ± 8 MeV, which makes it lighter than $B_1(5725)$. This makes it a natural candidate as the mixed light partner $|P_1'\rangle$, for which the predicted width is $\Gamma(B_1') = 219$ MeV; this result is compatible with the QCD sum rules prediction $\Gamma(B_1') \simeq 250$ MeV. As a test, we find that for $B_J^*(5732)$ as a

pure $^3P_1$ state its decay width is 153 MeV, which seems to agree well with the PDG suggested value. Whether $B_J^*(5732)$ is a mixed state $|P_1'\rangle$, a pure $^3P_1$ state, or another configuration needs further improved experimental measurement.

Similarly, for B_{s1} as a $|P_1\rangle$ state, its strong decay width and decay width ratio to the sum of B_{s1} and B_{2s}^* widths are

$$\Gamma(B_{s1}) \simeq 0.4 \sim 1 \text{ MeV}, \tag{45}$$

$$R \equiv \frac{\Gamma(B_{s1})}{\Gamma(B_{s1}) + \Gamma(B_{2s}^*)} = 0.02 \sim 0.6. \tag{46}$$

The predicted width $\Gamma(B_{s1})$ agrees with the data $\Gamma(B_{s1})_{\text{exp}} \sim 1$ MeV [77].

Since the mass of $|P_1'\rangle$ is slightly lower than that of $|P_1\rangle$, the mass of B_{s1}' (as a $|P_1'\rangle$ state) should be less than 5830 MeV. If we assume the mass of B_{s1}' is around 5830 MeV, this gives a broad decay width to the B^*K channel

$$\Gamma(B_{s1}') \simeq 149 \text{ MeV}. \tag{47}$$

We should point out that the mass of B_{s1}' is most likely below the threshold of B^*K; thus, the decay $B_{s1}' \to B^*K$ is kinematically forbidden. In this case the decay width of B_{s1}' will be very narrow. Its decay properties should be similar to those of $D_s(2460)$. The isospin violation decay $B_{s1}' \to B_s^*\pi$ and radiative decay $B_{s1}' \to B_s^*\gamma$ will be the dominant decay modes. A recent study of this scenario was given by Wang with light-cone sum rules [79].

C. Strong decays of 2S states

The radially excited heavy-light mesons are still not well established in experiments, although there are several candidates, such as $D^*(2640)^{\pm}$ [61], $D_{sJ}^*(2632)$ [62], and $D_{sJ}^*(2700)$ [6,7]. In theory, the radially excited D states 2^1S_0 and 2^3S_1 were predicted to have masses $\sim$2.58 and $\sim$2.64 GeV, respectively [21], while the radially excited D_s states 2^1S_0 and 2^3S_1 were $\sim$2.6 and $\sim$2.7 GeV, respectively [21,36]. In this section, we study the strong decays of these excited states into various channels. The mass uncertainties bring uncertainties into the predicted partial decay widths. Occasionally, some of the predicted partial widths exhibit sensitivities to the meson masses. Therefore, we present the strong decay widths of the D and D_s radially excited states as functions of their masses within a reasonable range as predicted by theory, and plot them along with their partial decay widths in Figs. 2 and 3, respectively. For a given initial mass, by comparing the relative magnitudes among different partial widths from theoretical prediction and experimental measurement, one can extract additional information about the initial meson quantum numbers.

1. Radially excited D mesons

For a 2^1S_0 state with a mass around 2.64 GeV, it can decay into $D^*\pi$, $D^*\eta$, D_s^*K, and $D_0^*(2400)\pi$. In Fig. 2, the partial widths and total strong decay width are shown for a mass range. In these channels, the $D^*\pi$ dominates the decays, the total decay width is $\sim$14 MeV at $m(D(2^1S_0)) = 2.58$ GeV, and it shows a flat behavior. Note that the threshold of the D_s^*K channel is very close to 2.64 GeV. Some sensitivities to this open channel thus occur in a mass range around 2.6 GeV. It shows that the D_s^*K width increases quickly with the masses and will compete against $D^*\eta$.

For the radially excited state 2^3S_1, its dominant decay channel is $D_1(2420)\pi$, while the other partial widths are much smaller (see the lower part of the right panel of Fig. 2). Again, the $D^*\pi$ partial width appears insensitive to the initial D meson mass.

Comparing the decay patterns between 2^1S_0 and 2^3S_1 in Fig. 2 is useful for clarifying $D^*(2640)^{\pm}$. This state was first seen by DELPHI in the $D^{*+}\pi^+\pi^-$ channel with a narrow width $<$15 MeV [61], but has not yet been confirmed by other experiments. If it is a genuine resonance, it will fit better into the 2^3S_1 state instead of 2^1S_0 due to its dominant decays into $D^{*+}\pi^+\pi^-$ which can occur via the main channel $D^*(2640)^+ \to D_1(2420)^0\pi^+$. In contrast, the assignment to a 2^1S_0 state will imply a dominant decay channel to $D^*\pi$, which is not supported by the data. Although the predicted width of $\sim$34 MeV overestimates

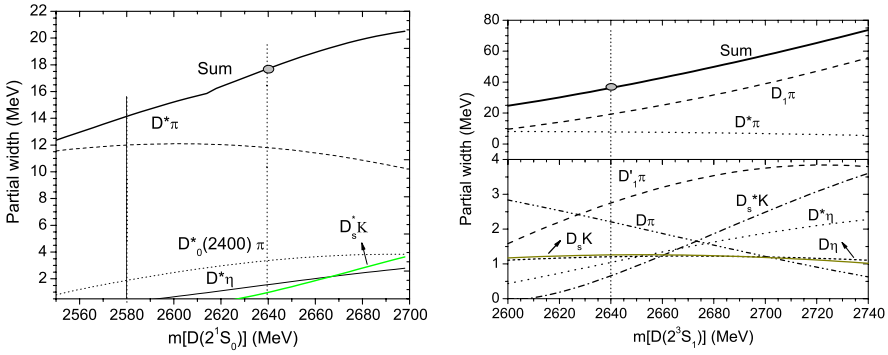

FIG. 2 (color online). The partial widths of $D(2^1S_0)$ and $D(2^3S_1)$ as functions of the mass.

the data by nearly a factor of 2, it should be more urgent to establish it in experiments and have a more precise measurement of its partial decay widths to both $D^*\pi$ and $D^*\pi\pi$.

2. Radially excited D_s mesons

There are experimental signals for several excited D_s states, i.e. $D_{sJ}(2632)$ [62], $D_{sJ}(2690)$, $D_{sJ}(2860)$ [6], and $D_{sJ}(2708)$ [7,80], for which the spectroscopic classification is still unsettled. The $D_{sJ}(2690)$ and $D_{sJ}(2708)$ are likely to be the same state as they have similar masses and both are broad. We shall compare these experimental observations with our model predictions in order to learn more about their spectroscopic classifications.

$D_{sJ}(2632)$ was reported by SELEX as a narrow state, i.e. $\Gamma < 17$ MeV, in $D_s\eta$ and DK channels [62]. The measured ratio of the partial widths is

$$R \equiv \frac{\Gamma(D^0K^+)}{\Gamma(D_s\eta)} = 0.16 \pm 0.06. \tag{48}$$

Its dominant decay into $D_s\eta$ makes it difficult to assign it into any simple $c\bar{q}$ scenario [81]. In particular, since a 2^1S_0 state is forbidden to decay into $D_s\eta$ and DK, this rules out $D_{sJ}(2632)$ to be a radially excited 0^-.

As shown by Fig. 3, the decay of a 2^3S_1 state turns out to be dominated by D^*K and possibly DK, while its decay into $D_s\eta$ is rather small. Therefore, a simple 2^3S_1 cannot explain its decay pattern as well. Some more investigations

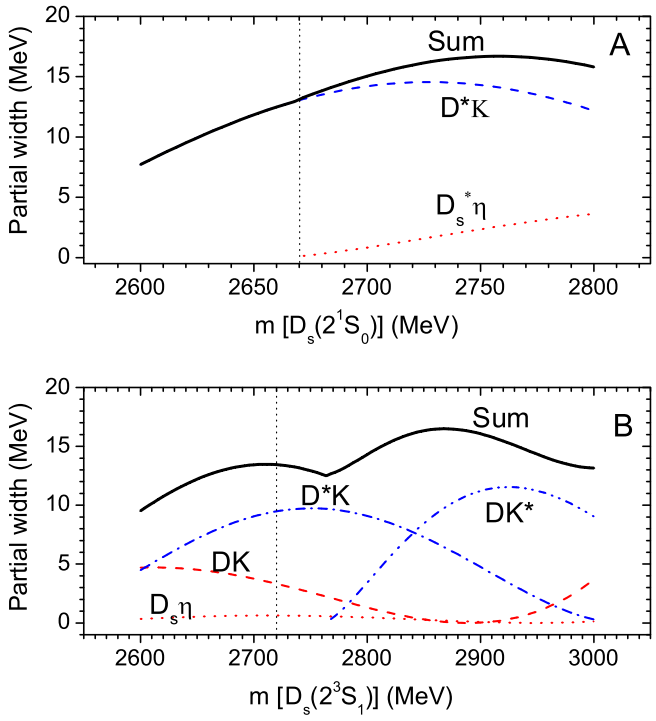

FIG. 3 (color online). The partial widths of $D_s(2^1S_0)$ and $D_s(2^3S_1)$ as functions of the mass.

of the nature of $D_{sJ}(2632)$ can be found in the literature, and here we restrict our attention to the output of our model calculations.

$D^*_{sJ}(2860)$ and $D^*_{sJ}(2690)$ from *BABAR* [6] [or $D_{sJ}(2708)$ from Belle [7,80]] have widths

$$\Gamma(D_{sJ}(2860)) = 48 \pm 17 \text{ MeV}, \tag{49}$$

$$\Gamma(D_{sJ}(2690)) = 112 \pm 43 \text{ MeV}, \tag{50}$$

and both are observed in the DK channel, and no evidence is seen in D^*K and $D_s\eta$ modes. Compare these with Fig. 3, which shows that neither of them can easily fit in 2^1S_0 or 2^3S_1.

By fixing the masses of 2^1S_0 and 2^3S_1 states as suggested by the quark model [36], i.e. $m(D_s(2^1S_0)) = 2.64$ GeV and $m(D_s(2^3S_1)) = 2.71$ GeV, we obtain their strong decay widths

$$\Gamma(D_s(2^1S_0)) \simeq 11 \text{ MeV}, \tag{51}$$

$$\Gamma(D_s(2^3S_1)) \simeq 14 \text{ MeV}, \tag{52}$$

which turn out to be narrow. For $D_s(2^1S_0)$, the predicted dominant decay mode is D^*K, while the DK channel is forbidden. For $D_s(2^3S_1)$, there are two main decay channels, D^*K and DK, and they give a ratio of

$$R \equiv \frac{\Gamma(D^*K)}{\Gamma(DK)} \simeq 2.6. \tag{53}$$

The $D_s\eta$ channel is also opened, but is negligibly small in comparison with DK and D^*K.

As $D^*_{sJ}(2860)$ has a relatively larger mass to fit in a D-wave state, we shall examine it with D-wave decays in the following subsection.

D. Strong decays of 1D states

Theoretical predicted masses of the D-wave excited D and D_s mesons are in a range of $2.8 \sim 2.9$ GeV [21,46]. To see the decay properties of those D-wave states, we plot their main decay partial widths in their possible mass region in Figs. 4 and 5 for D and D_s, respectively.

1. Excited D mesons

In Fig. 4, decays of four D-wave states are presented. It shows that the widths of $D(1^1D_2)$ and $D(1^3D_2)$ states are dominated by $D^*\pi$ decay, while the $D\pi/D\eta$ channels are forbidden. At $\sim$2.8 GeV, they have very broad widths larger than 300 MeV. As D^* dominantly decays into $D\pi$, such broad widths imply that their dominant final states are $D\pi\pi$, and it might be difficult to identify them in experiments. This may explain why these states are still evading experimental observations.

For $D(1^3D_1)$, $D^*\pi$ is also the main decay channel, but with a much smaller width. In contrast, $D\pi$ dominates the decay of $D(1^3D_3)$. With theory-suggested masses

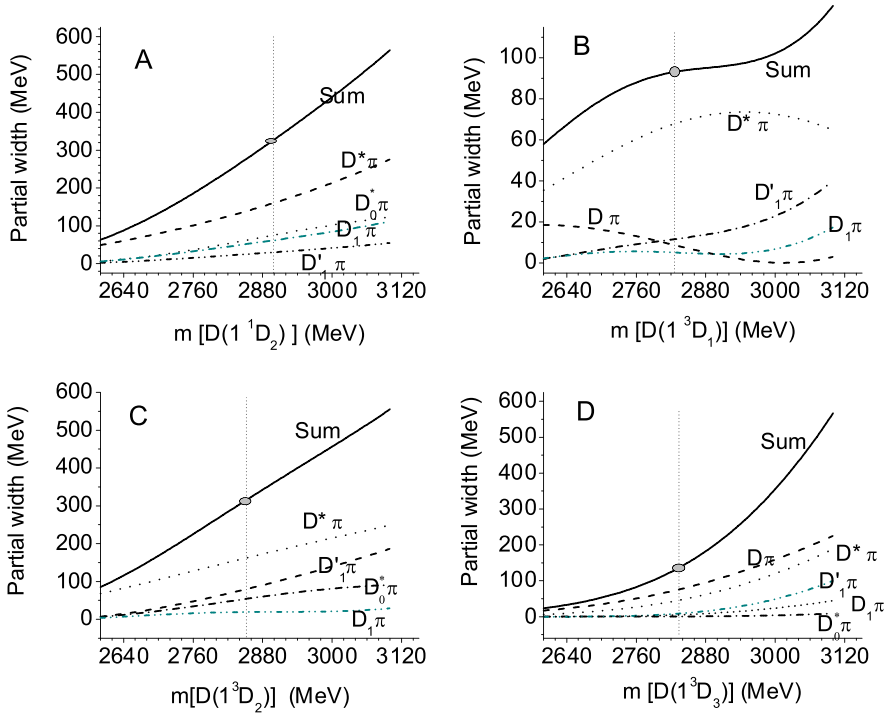

FIG. 4 (color online). The partial widths of $D(1^1D_2)$, $D(1^3D_1)$, $D(1^3D_2)$, and $D(1^3D_3)$ as functions of the mass.

$m(D(1^3D_1)) = 2.82$ and $m(D(1^3D_3)) = 2.83$ [21], the total pionic decay widths for $D(1^3D_1)$ and $D(1^3D_3)$ are predicted to be

$$\Gamma(D(1^3D_1)) \simeq 93 \text{ MeV}, \tag{54}$$

$$\Gamma(D(1^3D_3)) \simeq 130 \text{ MeV}, \tag{55}$$

and the predicted ratios between the $D^*\pi$ and $D\pi$ widths are

$$R(D(1^3D_1)) \equiv \frac{\Gamma(D\pi)}{\Gamma(D^*\pi)} \simeq 0.12, \tag{56}$$

$$R(D(1^3D_3)) \equiv \frac{\Gamma(D\pi)}{\Gamma(D^*\pi)} \simeq 1.7. \tag{57}$$

For $D(1^3D_3)$, the dominance of $D\pi$ decay suggests that it is relatively more accessible in experiments.

2. Excited D_s mesons

For $D_s(1^1D_2)$ and $D_s(1^3D_2)$, three important partial widths of D^*K, DK^*, and $D_s^*\eta$ are presented in Fig. 5, and both states are dominated by the D^*K decay. It is interesting to see that the mass of $\sim$2.8 GeV is about the threshold for DK^*. Although this decay mode is negligible near threshold, it can become important in case the masses for these two D-wave states are above 2.8 GeV.

At 2.8 GeV, the total widths are dominated by the D^*K mode, which are

$$\Gamma(D_s(1^1D_2)) \simeq 61 \text{ MeV}, \tag{58}$$

$$\Gamma(D_s(1^3D_2)) \simeq 84 \text{ MeV}. \tag{59}$$

These results can guide a search for these two states around 2.8 GeV.

As shown in Fig. 5, D^*K and DK are two dominant decay modes for $D_s(1^3D_1)$ if its mass is around 2.8 GeV, and the predicted width is relatively narrow. Implications from such an assignment will be discussed in Sec. V E.

Compared with the $D_s(1^3D_1)$ decay, the dominant decay mode of the $D_s(1^3D_3)$ state is DK around 2.8 GeV. With a higher mass the D^*K channel becomes increasingly important. This feature fits well the experimental observation for $D_{sJ}^*(2860)$, and makes it a possible assignment for this state.

To be more specific, for $D_{sJ}^*(2860)$ as a $D_s(1^3D_3)$ state, its predicted width is

$$\Gamma(D_s(1^3D_3)) \simeq 41 \text{ MeV}, \tag{60}$$

and the dominant decay mode is DK. In comparison, the decays via DK^* and $D_s\eta$ are much less important (see Fig. 5 and Table VIII). The ratio of DK and D^*K is found to be

$$R(D_s(1^3D_3)) \equiv \frac{\Gamma(DK)}{\Gamma(D^*K)} \simeq 2.3, \tag{61}$$

which is also consistent with the experiment [6]. This assignment agrees with results of Refs. [34,42,43].

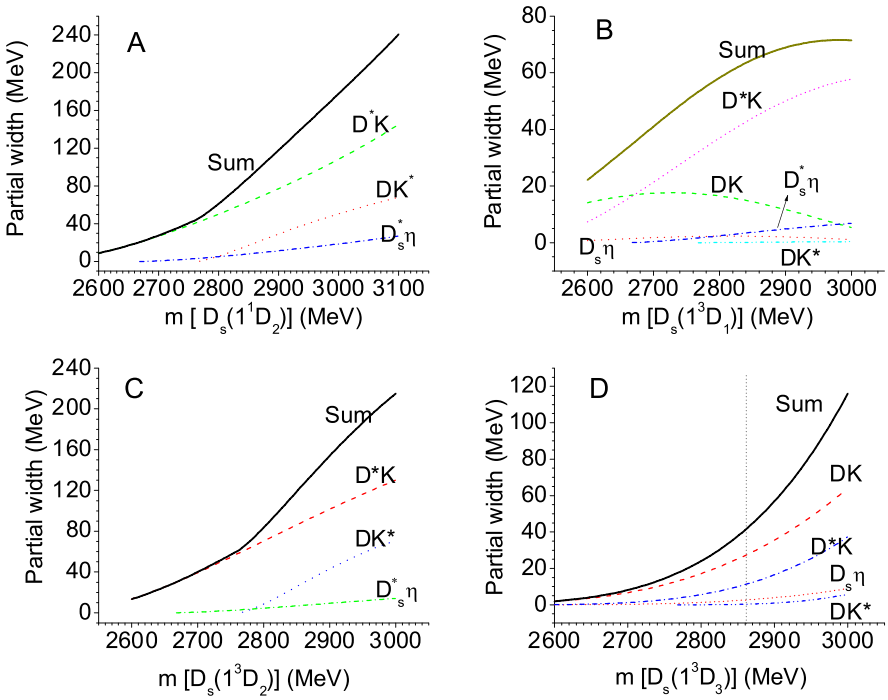

FIG. 5 (color online). The partial widths of $D_s(1^1D_2)$, $D_s(1^3D_1)$, $D_s(1^3D_2)$, and $D_s(1^3D_3)$ as functions of the mass. When we calculate the partial width of the DK^* channel, the D meson is looked at as the emitted pseudoscalar meson in the $SU(4)$ case [73].

Some models also suggested that $D^*_{sJ}(2860)$ could be a 2^3P_0 state [33,34,36], for which only decay mode DK and $D_s\eta$ are allowed. In our model, a 2^3P_0 state leads to decay amplitude

$$\mathcal{M}(2^3P_0 \to |1^1S_0\rangle\mathbb{P}) = i\frac{1}{4}\sqrt{\frac{1}{15}}g_1 F\frac{q'}{\alpha}\left[g^z_{10}\mathcal{G}q\frac{q'^2}{\alpha^2} - \frac{1}{3}g^z_{10}hq'\left(1+\frac{q'^2}{2\alpha^2}\right) - 2\sqrt{2}g^+_{10}hq'\left(7-\frac{q'^2}{\alpha^2}\right)\right] \quad (62)$$

with which its partial decay width to DK is about $\Gamma = 184$ MeV, and much broader than the experimental observation.

E. The 2^3S_1-1^3D_1 mixing

In Ref. [36], a mixing scheme between 2^3S_1 and 1^3D_1 was proposed as a solution for the relatively broad $D^*_{sJ}(2690)$, i.e.

$$|D^*_{s1}(2690)\rangle = \sin(\phi)|1^3D_1\rangle + \cos(\phi)|2^3S_1\rangle,$$
$$|D^*_{s1}(2810)\rangle = \cos(\phi)|1^3D_1\rangle - \sin(\phi)|2^3S_1\rangle, \quad (63)$$

where an orthogonal state $D^*_{s1}(2810)$ was also predicted. The mixing angle was found to favor $\phi = -0.5$ radians, i.e. $\phi \simeq -27°$. According to such a mixing scheme, $D^*_{s1}(2810)$ will also be a broad state and dominated by a 1^3D_1 configuration.

Taking the mixing scheme of Eq. (63), we plot the widths of $D^*_{sJ}(2690)$ and $D^*_{sJ}(2810)$ in terms of mixing angle ϕ in Fig. 6. The figure shows that if we take the mixing angle $\phi \simeq -27°$ as predicted in Ref. [36], the decay modes of $D^*_{sJ}(2690)$ are dominated by D^*K, which disagrees with the experimental observation. Nevertheless, the predicted decay width of $D^*_{sJ}(2690)$, $\Gamma \sim 25$ MeV, is underestimated by at least a factor of 2 compared with the data. If the $2S$-$1D$ mixing is small, e.g. $D^*_{sJ}(2690)$ is a pure

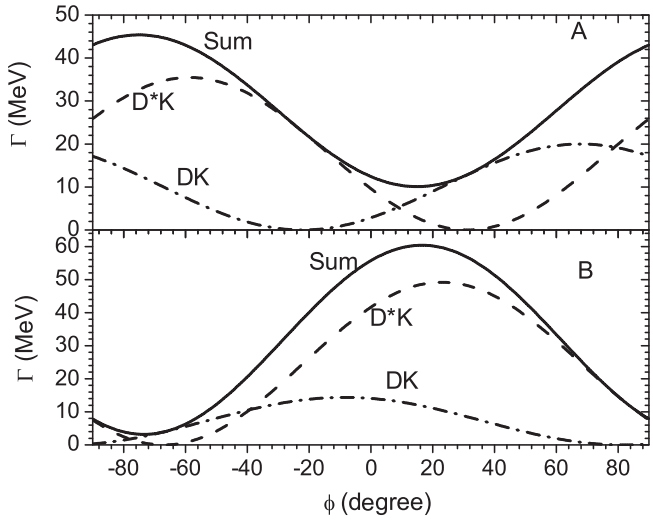

FIG. 6. The partial widths of low vector (A) and high vector (B) as functions of the mixing angle ϕ.

1^3D_1 state, the predicted decay width is $\Gamma \sim 42$ MeV, which is close to the lower limit of the data. However, the ratio $R = \Gamma(DK)/\Gamma(D^*K) \sim 0.8$ disagrees with the observation that the DK channel dominates the decay modes.

If we set $\phi \simeq 30°$, which implies that the sign of the spin-orbit splitting term is now negative to keep the correct mass ordering, the D^*K channel in the $D^*_{sJ}(2690)$ decay will be completely suppressed. This is consistent with the observations except that the decay width $\Gamma \sim 15$ MeV is too small to compare with the data.

For the high vector $D^*_{sJ}(2810)$, with $\phi \simeq \pm 30°$, its width reads $\sim$40–60 MeV and is dominated by the D^*K. Meanwhile, its branching ratio to DK is still sizeable.

Our test of the property of $D^*_{sJ}(2690)$ in the $2S$-$1D$ mixing scenario does not fit in the data very well. To clarify the nature of $D^*_{sJ}(2690)$, more accurate measurements of its width and ratio $R = DK/D^*K$, and experimental research for the accompanying $D^*_{sJ}(2810)$ in the DK and D^*K channels, are needed.

VI. SUMMARY

In the chiral quark model framework, we systematically study the strong decays of heavy-light mesons in $\mathbb{M} \to |1^1S_0\rangle\mathbb{P}$, $\mathbb{M} \to |1^3S_1\rangle\mathbb{P}$, $\mathbb{M} \to |1^3P_0\rangle\mathbb{P}$, $\mathbb{M} \to |1^1P_1\rangle\mathbb{P}$, and $\mathbb{M} \to |1^3P_1\rangle\mathbb{P}$. By adopting commonly used values for the constituent quark masses and pseudoscalar-meson decay constants, we make a full analysis of the strong decays of all the excited D^*, D^*_s, B^*, and B^*_s, and find that most available data can be consistently explained in this framework. We summarize our major results as follows.

A. Excited D mesons

The calculated partial decay widths for the $D^*(1^3S_1)$, $D^*_0(2400)$ as a 1^3P_0 state, and $D^*_2(2460)$ as a 1^3P_2 state are in good agreement with the data in our model and support their assignments as the low-lying excited D^*.

State mixing between the 1^1P_1 and 1^3P_1 is favored. With the mixing angle, $\phi \simeq -(55 \pm 5)°$, which is consistent with the prediction of Ref. [22], the narrow $D_1(2420)$ and broad $D'_1(2430)$ can be well explained as mixing states between 1^1P_1 and 1^3P_1. Precise measurement of the mass of the broad $D'_1(2430)$ is needed.

Our result shows that assigning $D^*(2640)$ to be a radially excited 2^3S_1 state can naturally explain its observation in the $D^{*+}\pi^+\pi^-$ final state, although the predicted width $\sim$34 MeV still possesses some discrepancies with the data. A search for the $D^*(2640)$ in the $D_1(2420)\pi$ channel is strongly recommended.

Although the $2S$ and $1D$ excited D states are still not well established, we analyzed their partial decay widths in their possible mass regions, which should be useful for future experimental studies. The decay widths of $2S$ states turn out to be narrow, namely, at the order of a few tens of MeV. Our results show that $D(2^1S_0)$ is dominated by the $D^*\pi$ decay channel, while both $D^*\pi$ and $D_1(2420)\pi$ are important for $D(2^3S_1)$. Both $D(1^1D_2)$ and $D(1^3D_2)$ have very broad widths $\gtrsim 300$ MeV, which may be difficult to identify in experiments. The decay widths of $D(1^3D_1)$ and $D(1^3D_3)$ are $\gtrsim 100$ MeV. The former has dominant decays into $D^*\pi$ and sizeable widths to $D\pi$ as well. For $D(1^3D_3)$, both $D\pi$ and $D^*\pi$ are important.

B. Excited D_s mesons

$D_s(2460)$ and $D_{s1}(2536)$ are identified as partners due to mixing between $^1P_1$ and $^3P_1$. With the mixing angle $\phi \simeq -(55 \pm 5)°$, our predictions for $D_{s1}(2536)$ are in good agreement with the data. Note that $D_s(2460)$ is below the strong decay threshold.

$D^*_{s2}(2573)$ is consistent with a 1^3P_2 state. Its partial decay width to DK is dominant while to D^*K is very small ($\sim$1 MeV). This explains its absence in the D^*K channel [74].

For those not-well-established states, by analyzing their decay properties, we find that $D^*_{sJ}(2860)$ strongly favors a $D_s(1^3D_3)$ state, while the $D^*_{sJ}(2632)$ and $D^*_{sJ}(2690)$ cannot fit in any pure D^*_s configurations.

For the unobserved $2S$ states, $D_s(2^1S_0)$ and $D_s(2^3S_1)$, their decay widths are predicted to be an order of $\sim$15 MeV, and dominated by the D^*K decay mode.

For the unobserved $1D$ states, $D_s(1^1D_2)$, $D_s(1^3D_2)$, and $D_s(1^3D_1)$, their decay widths are of the order of $60 \sim 80$ MeV at a mass of $\sim$2.8 GeV. The $D_s(1^1D_2)$ and $D_s(1^3D_2)$ decay widths are dominated by the D^*K mode, while $D_s(1^3D_1)$ is dominated by the D^*K and DK together.

C. Excited B mesons

We also study the decay properties of the newly observed bottom states $B_1(5725)$, $B^*_2(5829)$. Our calculations strongly suggest that $B_1(5725)$ is a mixed $|P_1\rangle$ state, and $B^*_2(5829)$ satisfies an assignment of 1^3P_2.

The $B^*_J(5732)$, which was first reported by the L3 Collaboration, can be naturally explained as the broad partner ($|P'_1\rangle$) of $B_1(5725)$ in the $^1P_1$ and $^3P_1$ mixing scheme. Its predicted width is $\Gamma(B'_1) = 219$ MeV, which is larger than the PDG suggested value $\Gamma_{\rm exp} = 128 \pm 18$ MeV. In contrast, as a pure 1^3P_1 state, its decay width is $\Gamma(B'_1) = 153$ MeV. Whether $B^*_J(5732)$ is a mixed state $|P'_1\rangle$, a pure 1^3P_1 state, or other configuration should be further studied.

The theoretical prediction of the mass for the $B^*_0(^3P_0)$ meson is about 5730 MeV. Its decay into $B\pi$ has a broad width $\Gamma(B^*_0) = 272$ MeV according to our prediction.

D. Excited B_s mesons

The two new narrow bottom-strange mesons $B_{s1}(5830)$ and $B^*_{s2}(5839)$ observed by CDF are likely the mixed state

P_1 and the 1^3P_2 state, respectively, though their decay widths and ratios are not given. For $B_{s1}(5830)$ as a $|P_1\rangle$ state, its predicted width and decay ratio are $\Gamma(B_{s1}) \simeq (0.4 \sim 1)$ MeV and $\Gamma(B_{s1})/(\Gamma(B_{s1}) + \Gamma(B^*_{2s})) = 0.02 \sim 0.6$. For $B_s(5839)$ as the $^3P_2$ state, its decay width and width ratio predicted by us are $\Gamma(B^*_{s2}) \simeq 2$ MeV and $\Gamma(B^*K)/\Gamma(BK) \simeq 6\%$.

The theoretical prediction for the B^*_{s0} mass is about 5800 MeV. In our model it has a broad width $\Gamma(B^*_0) = 227$ MeV. For B'_{s1} if its mass is above the threshold of B^*K, it will be a broad state with $\Gamma(B'_{s1}) \simeq 149$ MeV. Otherwise, it should be a narrow state.

It should be mentioned that uncertainties with quark model parameters can give rise to uncertainties with the theoretical results. A qualitative examination shows that such uncertainties can be as large as 10%–20%, which are a typical order for quark model approaches. Interestingly, systematics arising from such a simple prescription are useful for us to gain insights into the effective degrees of freedom inside those heavy-light mesons and the underlying dynamics for their strong decays.

ACKNOWLEDGMENTS

The authors wish to thank F. E. Close and S.-L. Zhu for useful discussions. This work is supported, in part, by the National Natural Science Foundation of China (Grants 10675131 and 10775145), Chinese Academy of Sciences (KJCX3-SYW-N2), the U.K. EPSRC (Grant No. GR/S99433/01), the Post-Doctoral Programme Foundation of China, and K. C. Wong Education Foundation, Hong Kong.

[1] B. Aubert *et al.* (*BABAR* Collaboration), Phys. Rev. Lett. **90**, 242001 (2003).
[2] B. Aubert *et al.* (*BABAR* Collaboration), Phys. Rev. D **69**, 031101 (2004).
[3] D. Besson *et al.* (CLEO Collaboration), Phys. Rev. D **68**, 032002 (2003); **75**, 119908(E) (2007).
[4] Y. Mikami *et al.*, Phys. Rev. Lett. **92**, 012002 (2004).
[5] P. Krokovny *et al.* (Belle Collaboration), Phys. Rev. Lett. **91**, 262002 (2003).
[6] B. Aubert (*BABAR* Collaboration), Phys. Rev. Lett. **97**, 222001 (2006).
[7] J. Brodzicka *et al.* (Belle Collaboration), Phys. Rev. Lett. **100**, 092001 (2008).
[8] CDF Collaboration, CDF Note 8945, 2007.
[9] V. M. Abazov *et al.* (D0 Collaboration), Phys. Rev. Lett. **99**, 172001 (2007).
[10] T. Aaltonen *et al.* (CDF Collaboration), Phys. Rev. Lett. **100**, 082001 (2008).
[11] V. Abazov *et al.* (D0 Collaboration),, Phys. Rev. Lett. **100**, 082002 (2008).
[12] S. Bianco, in *Hadron Spectroscopy: Eleventh International Conference on Hadron Spectroscopy*, AIP Conf. Proc. No. 814 (AIP, New York, 2006), p. 24.
[13] I. Kravchenko (CDF Collaboration), arXiv:hep-ex/0605076.
[14] R. Waldi, arXiv:hep-ex/0703043.
[15] A. Zghiche (*BABAR* Collaboration), arXiv:0710.0314.
[16] V. Poireau, arXiv:0711.3683.
[17] R. K. Mommsen, Nucl. Phys. B, Proc. Suppl. **170**, 172 (2007).
[18] M. Kreps (CDF Collaboration), arXiv:0711.4890.
[19] F. E. Close and E. S. Swanson, Phys. Rev. D **72**, 094004 (2005).
[20] S. Godfrey, Phys. Rev. D **72**, 054029 (2005).
[21] S. Godfrey and N. Isgur, Phys. Rev. D **32**, 189 (1985).
[22] S. Godfrey and R. Kokoski, Phys. Rev. D **43**, 1679 (1991).
[23] N. Isgur and M. B. Wise, Phys. Rev. Lett. **66**, 1130 (1991).
[24] M. Di Pierro and E. Eichten, Phys. Rev. D **64**, 114004 (2001).
[25] E. J. Eichten, C. T. Hill, and C. Quigg, Phys. Rev. Lett. **71**, 4116 (1993).
[26] A. F. Falk and T. Mehen, Phys. Rev. D **53**, 231 (1996).
[27] K. O. E. Henriksson, T. A. Lahde, C. J. Nyfalt, and D. O. Riska, Nucl. Phys. **A686**, 355 (2001).
[28] N. Tregoures and W. Roberts, Phys. Rev. D **61**, 074032 (2000).
[29] J. L. Goity and W. Roberts, Phys. Rev. D **60**, 034001 (1999).
[30] S. L. Zhu and Y. B. Dai, Mod. Phys. Lett. A **14**, 2367 (1999).
[31] Y. B. Dai and S. L. Zhu, Phys. Rev. D **58**, 074009 (1998).
[32] A. H. Orsland and H. Hogaasen, Eur. Phys. J. C **9**, 503 (1999).
[33] E. Van Beveren and G. Rupp, Phys. Rev. Lett. **97**, 202001 (2006).
[34] B. Zhang, X. Liu, W. Z. Deng, and S. L. Zhu, Eur. Phys. J. C **50**, 617 (2007).
[35] W. Wei, X. Liu, and S. L. Zhu, Phys. Rev. D **75**, 014013 (2007).
[36] F. E. Close, C. E. Thomas, O. Lakhina, and E. S. Swanson, Phys. Lett. B **647**, 159 (2007).
[37] P. Colangelo, F. De Fazio, S. Nicotri, and M. Rizzi, Phys. Rev. D **77**, 014012 (2008).
[38] Z. G. Wang, arXiv:0708.0155.
[39] F. K. Guo, P. N. Shen, and H. C. Chiang, Phys. Lett. B **647**, 133 (2007).
[40] A. Faessler, T. Gutsche, V. E. Lyubovitskij, and Y. L. Ma, Phys. Rev. D **77**, 114013 (2008).
[41] S. Yasui and M. Oka, Phys. Rev. D **76**, 034009 (2007).
[42] P. Colangelo, F. De Fazio, and S. Nicotri, Phys. Lett. B **642**, 48 (2006).
[43] J. Koponen (UKQCD Collaboration), arXiv:0708.2807.
[44] J. Vijande, F. Fernandez, and A. Valcarce, J. Phys. G **31**, 481 (2005).

[45] J. Vijande, F. Fernandez, and A. Valcarce, Phys. Rev. D **73**, 034002 (2006); **74**, 059903(E) (2006).
[46] T. Matsuki, T. Morii, and K. Sudoh, Prog. Theor. Phys. **117**, 1077 (2007).
[47] J. Vijande, A. Valcarce, and F. Fernandez, Phys. Rev. D **77**, 017501 (2008).
[48] D. M. Li, B. Ma, and Y. H. Liu, Eur. Phys. J. C **51**, 359 (2007).
[49] E. S. Swanson, in *Quark Confinement and the Hadron Spectrum VII: Seventh Conference on Quark Confinement and the Hadron Spectrum*, AIP Conf. Proc. No. 892 (AIP, New York, 2007), p. 362; J. Phys. Conf. Ser. **69**, 012007 (2007).
[50] D. Ebert, V. O. Galkin, and R. N. Faustov, Phys. Rev. D **57**, 5663 (1998); **59**, 019902(E) (1999).
[51] T. Barnes, in *Hadron Spectroscopy: Eleventh International Conference on Hadron Spectroscopy*, AIP Conf. Proc. No. 814 (AIP, New York, 2006), p. 735.
[52] E. Swanson, in *Hadron Spectroscopy: Eleventh International Conference on Hadron Spectroscopy*, AIP Conf. Proc. No. 814 (AIP, New York, 2006), p. 203; Int. J. Mod. Phys. A **21**, 733 (2006).
[53] E. S. Swanson, Phys. Rep. **429**, 243 (2006).
[54] J. L. Rosner, J. Phys. G **34**, S127 (2007).
[55] S. L. Zhu, Nucl. Phys. **A805**, 221C (2008).
[56] J. L. Rosner, J. Phys. Conf. Ser. **69**, 012002 (2007).
[57] S. Nicotri, in *QCD@Work 2007: International Workshop on Quantum Chromodynamics; Theory and Experiment*, AIP Conf. Proc. No. 964 (AIP, New York, 2007), p. 137.
[58] E. Klempt and A. Zaitsev, Phys. Rep. **454**, 1 (2007).
[59] P. Colangelo, F. De Fazio, R. Ferrandes, and S. Nicotri, Prog. Theor. Phys. Suppl. **168**, 202 (2007).
[60] B. Ananthanarayan, S. Banerjee, K. Shivaraj, and A. Upadhyay, Phys. Lett. B **651**, 124 (2007).
[61] P. Abreu *et al.* (DELPHI Collaboration), Phys. Lett. B **426**, 231 (1998).
[62] A. V. Evdokimov *et al.* (SELEX Collaboration), Phys. Rev. Lett. **93**, 242001 (2004).
[63] A. Manohar and H. Georgi, Nucl. Phys. **B234**, 189 (1984).
[64] T. Abdullah and F. E. Close, Phys. Rev. D **5**, 2332 (1972).
[65] F. E. Close and Z. P. Li, Phys. Rev. D **42**, 2194 (1990).
[66] Z. P. Li, Phys. Rev. D **48**, 3070 (1993); **50**, 5639 (1994); **52**, 4961 (1995); Phys. Rev. C **52**, 1648 (1995).
[67] Z. P. Li, H. X. Ye, and M. H. Lu, Phys. Rev. C **56**, 1099 (1997).
[68] Q. Zhao, J. S. Al-Khalili, and C. Bennhold, Phys. Rev. C **64**, 052201 (2001).
[69] Q. Zhao, J. S. Al-Khalili, Z. P. Li, and R. L. Workman, Phys. Rev. C **65**, 065204 (2002).
[70] Q. Zhao, B. Saghai, and Z. P. Li, J. Phys. G **28**, 1293 (2002).
[71] Q. Zhao, Z. P. Li, and C. Bennhold, Phys. Rev. C **58**, 2393 (1998); Phys. Lett. B **436**, 42 (1998).
[72] X. H. Zhong, Q. Zhao, J. He, and B. Saghai, Phys. Rev. C **76**, 065205 (2007).
[73] X. H. Zhong and Q. Zhao, Phys. Rev. D **77**, 074008 (2008).
[74] Y. M. Yao *et al.* (Particle Data Group), J. Phys. G **33**, 1 (2006).
[75] K. Abe *et al.* (Belle Collaboration), Phys. Rev. D **69**, 112002 (2004).
[76] J. M. Link *et al.* (FOCUS Collaboration), Phys. Lett. B **586**, 11 (2004).
[77] R. Akers *et al.* (OPAL Collaboration), Z. Phys. C **66**, 19 (1995).
[78] V. Balagura *et al.* (Belle Collaboration), Phys. Rev. D **77**, 032001 (2008).
[79] Z. G. Wang, arXiv:0803.1223.
[80] K. Abe *et al.* (Belle Collaboration), arXiv:hep-ex/0608031.
[81] T. Barnes, F. E. Close, J. J. Dudek, S. Godfrey, and E. S. Swanson, Phys. Lett. B **600**, 223 (2004).